32nd URSI GASS, Montreal, 19–26 August 2017

Study on the Accuracy of Forward Modeling in Electrical Impedance Tomography for Thorax Imaging

Ke Zhang*(1), Maokun Li(1), Fan Yang(1), Shenheng Xu(1), and Aria Abubakar(2)
(1) State Key Laboratory on Microwave and Digital Communications,
Tsinghua National Laboratory for Information Science and Technology,
Department of Electronic Engineering, Tsinghua University, Beijing 100084, China
(2) Schlumberger, Sugar Land, Texas, 77478, USA

Abstract

In this paper, we study the data calibration procedure in electrical impedance tomography (EIT) for thorax imaging. Data calibration is an important procedure in EIT imaging as it bridges the gap between simulated data and measured data. Minimizing the systematic error caused by forward modeling could significantly improve the quality of reconstruction. A few factors are investigated in this study including: 1) electrode model; 2) skin impedance; 3) dimensionality of forward modeling. We observe that the dimensionality of forward modeling is the most critical factor. In fact, simulated data comparable with the experimental data can be obtained using three-dimensional forward modeling and reasonable estimation of background conductivity. It can serve as a good starting point for EIT data inversion. Finally, we perform a fully three-dimensional reconstruction using the measured data of human pulmonary ventilation. The reconstructed images further support our conclusion.

1 Introduction

Electrical impedance tomography (EIT) is a non-invasive, real-time and radiation-free imaging technique with many promising clinical applications [1]. In particular, EIT is an excellent tool for monitoring pulmonary ventilation. In EIT measurement, an array of electrodes is attached to human chest. As currents are injected to human body through one pair of electrodes, voltages on other electrodes are measured. Conductivity distribution of human chest can then be reconstructed from the measured data. Because lung conductivity is affected by the air portion inside it, changes in conductivity reflect the dynamics of human breath.

In order to improve the quality of reconstruction, a rigorous forward modeling is usually preferred. In [2], error factors such as the boundary shape, electrode sizes and locations, and contact impedance are assessed by the observation on 2D reconstructions using synthetic data. In [3], error factors such as the electrode sizes and placement, mesh density, and selection of reference conductivity are discussed in detail and the importance of using 3D forward models is stressed. In [4], the impacts of electrode area, contact impedance and boundary shape on reconstructions are investigated by 2D simulations and the artifacts observed in images are quantified. While incorporation of the above factors improves the accuracy of forward modeling, it also increases the complexity of forward model computation. Therefore, most of equipments used clinically these days are still based on 2D thorax modeling and inversion methods, and the reconstructed images are only used for qualitative evaluation. In order to further improve the accuracy of reconstruction and enable quantitative evaluation, we need to quantify the improvements in accuracy from modeling the above factors. Considering the time constraint from realtime monitoring, determining the dominant factors will help us to achieve a good balance between accuracy and computational complexity.

In this paper, we study a variety of factors affecting the accuracy of forward modeling including: electrode model (point electrode model or complete electrode model), skin impedance and dimensionality of forward modeling (2D or 3D). The assessment of these factors is by comparing the simulated data concerning each of them with the experimental data acquired from human lung ventilation measurement, instead of by observing the reconstructed images, which is intuitive but indirect. The paper is organized as follows: In Section 2, a brief review is made on the forward modeling in EIT. Then the measurement setup is introduced and the experimental data is presented. In Section 3, the three considered factors mentioned above are introduced respectively, and the simulated data are compared with the experimental data. In Section 4, the data calibration results are validated by a test reconstruction using experimental data. In Section 5, a conclusion is drawn on factors affecting the accuracy of EIT forward modeling and a summary is made on the limitations of current work.

2 Forward Modeling in EIT and Experimental Data

The electric potential in the domain of investigation $\Omega \subset \mathbf{R}^n$ ($n = 2$ or 3) satisfies the Poisson's equation

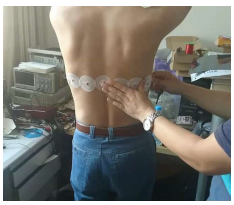

(a) Measurement setup

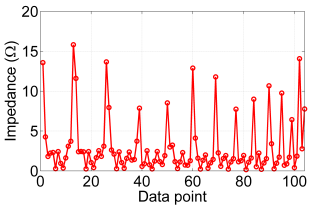

(b) A frame of measured data

Figure 1. (a) Measurement setup. (b) A frame of data measured at the end of expiration. The data is normalized with the injected currents and has a unit of impedance.

$$\bigtriangledown \cdot (\sigma(\mathbf{r}) \bigtriangledown \phi(\mathbf{r})) = 0 \quad \mathbf{r} \in \Omega, \tag{1}$$

where σ is the conductivity distribution, ϕ is the electric potential and $\mathbf{r}$ is the spatial position. In order to solve the partial differential equation in (1), certain boundary conditions are needed. These boundary conditions define the current density or the potential on the boundary $\partial\Omega$. The governing equation (1) together with the boundary conditions is usually called an electrode model. Details of several electrode models will be discussed in Section 3.1.

In the implementation, the problem domain Ω is generally discretized using triangular meshes in 2D or tetrahedral meshes in 3D, and the boundary-value problem mentioned above is solved by finite element method (FEM).

In real measurement, we use a 16-electrode EIT system operating at 20 kHz. The electrodes are equally spaced around the subject's thorax, as shown in Figure 1 (a). Constant currents are injected between adjacent electrodes and voltages are measured between non-current-carrying adjacent electrodes. Therefore, a frame of data contains 104 data points. Figure 1 (b) shows a frame of data measured at the end of expiration.

3 Study on Influence Factors in Forward Modeling

3.1 Electrode Model

In the measurement, we use circular ECG electrodes consisting of Ag/AgCl conductor and gel pad with diameters of 7.5mm and 16mm respectively. The skin is cleaned using alcohol before the electrodes are attached.

Among various electrode models designed for FEM modeling [5], one widely used is the complete electrode model (CEM). The details of CEM can be found in [6]. In point electrode model (PEM), the electrodes are represented by a series of points $\mathbf{r}_\ell (\ell = 1, 2, ..., L)$ (L is the number of electrodes) on the boundary $\partial\Omega$. In this model, the normal current density on the boundary is non-zero only at the electrode points, which leads to a δ-like normal current density distribution on the boundary:

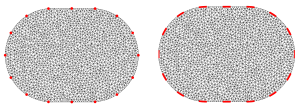

(a) Model 1

(b) Model 2

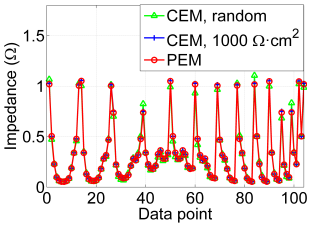

(c) Comparison

Figure 2. (a) PEM thorax model. (b) CEM thorax model. (c) For CEM, the contact impedance is modeled in two cases: 1) 1000 Ω·cm^2 for all the electrodes; 2) 1% random variation around 1000 Ω·cm^2 for the electrodes.

$$\sigma(\mathbf{r}) \frac{\partial \phi(\mathbf{r})}{\partial n} = \sum_{\ell=1}^{L} I_\ell \delta(\mathbf{r} - \mathbf{r}_\ell), \quad \mathbf{r} \in \partial\Omega, \tag{2}$$

where n is the outward normal direction on $\partial\Omega$ and I_ℓ is the injected current on Electrode ℓ. Then considering the conservation of charge condition

$$\sum_{\ell=1}^{L} I_\ell = 0, \tag{3}$$

and the choice of a reference potential

$$\int_{\partial\Omega} \phi(\mathbf{r}) d\mathbf{r} = 0. \tag{4}$$

We note that the point electrode model is only a simplified model when the electrodes used are small as in our case, and it may be a poor model when large electrodes are used.

We solve the forward problem using PEM and CEM respectively by finite element method [7]. Two simple two-dimensional finite-element thorax models are shown in Figure 2 (a) and (b). The two models correspond to PEM and CEM respectively. In the simulation, we use a homogeneous conductivity of 0.1 S/m, which is a reasonable background conductivity of human thorax at 20 kHz [8]. In addition, proper contact impedance of the electrodes needs to be chosen when CEM is used. Rosell *et al.* [9] report a measured contact impedance of about 1000 Ω·cm^2 at 20 kHz. Hence, we simulate the case where all the electrodes have the same contact impedance of 1000 Ω·cm^2 and the case where the contact impedance has a 1% random variation around 1000 Ω·cm^2. A comparison of simulated results using PEM and CEM is shown in Figure 2 (c), from which we can see the simulated data using CEM is only slightly different from that of PEM, and both are not in the same order of magnitude as the experimental data (see Figure 1 (b)). Therefore, more factors need to be investigated for accurate forward modeling.

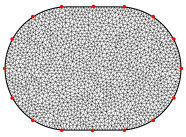

(a) Model 3

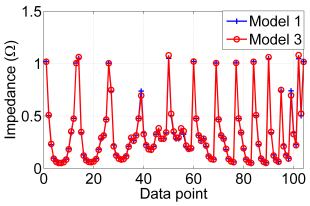

(b) Comparison

Figure 3. (a) A model with a thin layer of skin (about 1.25 mm thick). The skin layer has a conductivity of 2×10^{-4} S/m and the interior area has a conductivity of 0.1 S/m. (b) Comparison of simulated data using non-skin model (Model 1) and skin model (Model 3).

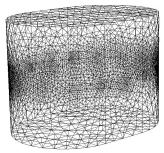

(a) Model 4

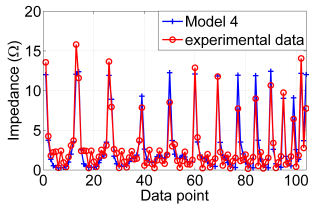

(b) Comparison

Figure 4. (a) A three-dimensional thorax model constructed using NETGEN. (b) Comparison of experimental data and simulated data using Model 4. Homogeneous conductivity of 0.1 S/m is used in the simulation.

3.2 Skin Impedance

The skin impedance is mainly caused by the stratum corneum and may have large spatial and temporal variation. It is reported that dry skin has a resistivity of about 5×10^3 Ω·m and wet skin has a resistivity of about 2.5×10^2 Ω·m, both at 20 kHz and 37 °C [8]. The skin resistivity is very different from that of the inclusions of thorax.

Skin impedance can be incorporated in the contact impedance [2], but here we model it independently. To test the influence of highly resistive skin on the accuracy of forward modeling, we construct a model (Model 3) including a thin layer of skin, as shown in Figure 3 (a). The model is equipped with point electrodes in order to highlight the influence of skin impedance. The thickness of the skin layer is about 1.25 mm (an average thickness of the skin) and the resistivity of the skin layer is chosen at the worst case scenario of 5×10^3 Ω·m. The simulated data using the non-skin model (Model 1) and the skin model (Model 3) is shown in Figure 3 (b), from which we can see the skin layer has little influence on the simulated data and it also fails to interprete the experimental data (see Figure 1 (b)).

3.3 Dimensionality of Forward Modeling

In the previous discussions, two-dimensional models (Model 1–Model 3) are used in forward modeling. This is mainly because all the electrodes are located on one plane and most injected currents flow near this plane. Moreover, 2D modeling has much less unknowns compared with 3D modeling, which is advantageous for realtime applications such as pulmonary ventilation monitoring.

However, in measurements of human ventilation, the injected currents flow in three dimensions, not purely confined in the two-dimensional electrode plane. This phenomenon becomes more obvious when small and circular electrodes are used. Hence it is necessary to compare the accuracy of forward modeling between two- and three-dimensional models. To this end, we construct a three-dimensional thorax model (Model 4) using NETGEN, as shown in Figure 4 (a). The model consists of 49327 tetrahedral elements and 9989 nodes. For simplicity, point electrode model depicted in Section 3.1 is used. The comparison of the experimental data and the simulated data using Model 4 is shown in Figure 4 (b), from which we can see the scale of simulated data is comparable with the one of experimental data. Therefore, we can conclude that the dimensionality of forward modeling is the most critical one to the accuracy of EIT forward modeling among all the three factors studied in this paper.

4 Reconstruction Test

Through the previous study, we observe that better reconstruction may be obtained using three-dimensional forward modeling. In this section we perform a linearized three-dimensional difference reconstruction [10] using the experimental data of lung ventilation to further verify this observation. Homogeneous conductivity of 0.1 S/m is used to calculate the Jacobian matrix. The selection of 0.1 S/m is based on two considerations: 1) the simulated data using 0.1 S/m is close to the experimental data, as can be seen from Figure 4 (b); 2) the conductivity 0.1 S/m is a reasonable background conductivity of the human thorax [8]. The reconstructed conductivity image is shown in Figure 5 (a). For clarity, we only show the reconstruction on the electrode plane, where the conductivity of each triangular element is approximated by the average conductivity of the two tetrahedral elements related to it. As a comparison, the two-dimensional reconstruction result is also shown in Figure 5 (b) where the Jacobian is calculated using two-dimensional forward modeling. It is obvious that the three-dimensional reconstruction result is more reasonable compared with human thorax structure as shown in a CT image in Figure 5 (c). The reconstruction results validate our observation in the previous section that dimensionality is the most important factor in the accuracy of forward modeling.

5 Conclusion and Discussion

In this paper we study the influence of electrode model, skin impedance and model dimensionality on the accuracy of forward modeling of EIT in monitoring human pulmonary ventilation. The results show that all these three factors

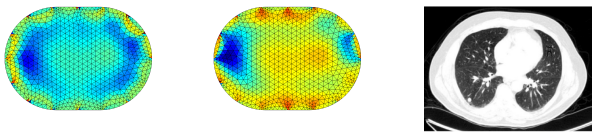

(a) 3D reconstruction (b) 2D reconstruction (c) A CT image

Figure 5. Reconstruction results. (a) A fully 3D reconstruction using 3D model. Only the reconstruction of the electrode plane is shown. (b) A fully 2D reconstruction using the mesh extracted from the electrode plane of the 3D model. (c) An example of CT image of human thorax.

have some influence on the simulated data, but the dimensionality of forward modeling is the most critical one. In fact, simulated data comparable with the experimental data can be obtained using three-dimensional forward modeling. Finally, a three-dimensional reconstruction test using the experimental data further validates our observation.

There are still some limitations of our work:

- In the two-dimensional simulation using complete electrode model, the values of contact impedance used are from the literature. This is only a rough approximation because the contact impedance is likely to change due to the different subject and measurement environment.
- In the study of skin impedance, we use a rather ideal model for the skin with the same thickness and resistivity. In fact, the skin impedance may have spatial and temporal variation and this may affect the forward modeling.
- The three-dimensional forward modeling uses the point electrode model and the contact impedance is not considered. For more exact forward modeling, the complete electrode model should be used.

In addition, other factors such as the boundary shape, electrode sizes and electrode locations may also have some effects on the accuracy of forward modeling and this calls for more exact modeling techniques. We will investigate them in our future research.

6 Acknowledgements

The authors would like to thank the support from National Science Foundation of China under contract 61571264 and from Tsinghua National Laboratory for Information Science and Technology under contract 042003212.

References

[1] Eduardo L. V. Costa, Raul Gonzalez Lima and Marcelo B. P. Amato, "Electrical Impedance Tomography," *Intensive Care Medicine: Annual Update 2009*, 2009, pp. 394–404, doi:10.1007/978-0-387-92278-2_38.

[2] V. Kolehmainen, M. Vauhkonen, P. A. Karjalainen and J. P. Kaipio, "Assessment of Errors in Static Electrical Impedance Tomography with Adjacent and Trigonometric Current Patterns," *Physiological Measurement*, **18**, 4, 1997, pp. 289–303, doi: 10.1088/0967-3334/18/4/003.

[3] Andy Adler, John H. Arnold, Richard Bayford, Andrea Borsic, Brian Brown, Paul Dixon, Theo J. C. Faes, InÃl'z Frerichs, HervÃl' Gagnon, Yvo GÃd'rber, BartÅĆomiej Grychtol, GÃijnter Hahn, William R. B. Lionheart, Anjum Malik, Robert P. Patterson, Janet Stocks, Andrew Tizzard, Norbert Weiler and Gerhard K. Wolf, "GREIT: a Unified Approach to 2D Linear EIT Reconstruction of Lung Images," *Physiological Measurement*, **30**, 6, June 2009, pp. S35–S55, doi: 10.1088/0967-3334/30/6/s03.

[4] A. Boyle and A. Adler, "The Impact of Electrode Area, Contact Impedance and Boundary Shape on EIT Images," *Physiological Measurement*, **32**, 7, 2011, pp. 745–754, doi: 10.1088/0967-3334/32/7/S02.

[5] M. Cheney, D. Isaacson and J. C. Newell, "Electrical Impedance Tomography," *SIAM Review*, **41**, 1, Sept 1999, pp. 85–101, doi: 10.1137/S0036144598333613.

[6] Kuo-Sheng Cheng , D. Isaacson , J. C. Newell and D. G. Gisser, "Electrode Models for Electric Current Computed Tomography," *IEEE Transactions on Biomedical Engineering*, **36**, 9, Sept 1989, pp. 918–924, doi: 10.1109/10.35300.

[7] M. Soleimani, C. E. Powell and N. Polydorides, "Improving the Forward Solver for the Complete Electrode Model in EIT Using Algebraic Multigrid," *IEEE Transactions on Medical Imaging*, **24**, 5, May 2005, pp. 577–583, doi: 10.1109/TMI.2005.843741.

[8] S. Gabriel, R. W. Lau and C. Gabriel, "The Dielectric Properties of Biological Tissues: III. Parametric Models for the Dielectric Spectrum of Tissues," *Physics in Medicine and Biology*, **41**, 11, Nov 1996, pp. 2271–2293, doi: 10.1088/0031-9155/41/11/003.

[9] Javier Rosell, Josep Colominas, Pere Riu, Ramon Pallas-Areny and John G. Webster, "Skin Impedance From 1 Hz to 1 MHz," *IEEE Transactions on Biomedical Engineering*, **35**, 8, Sept 1988, pp. 649–651, doi: 10.1109/10.4599.

[10] A. Adler, R. Gaburro and W. Lionheart, "Electrical Impedance Tomography," *Handbook of Mathematical Methods in Imaging*, Springer New York, 2011, pp. 599–654, doi: 10.1007/978-0-387-92920-0.